ELSEVIER

Hydrothermal synthesis, structure and thermal stability of diamine templated layered uranyl-vanadates

Murielle Rivenet*, Nicolas Vigier, Pascal Roussel, Francis Abraham

*Unité de Catalyse et de Chimie du Solide, Equipe Chimie du Solide, UCCS UMR CNRS 8181, USTL, ENSC-B.P. 90108,
59652 Villeneuve d'Ascq Cedex, France*

Abstract

Six new layered uranyl vanadates $(NH_4)_2[(UO_2)_2V_2O_8]$ (**1**), $(H_2EN)[(UO_2)_2V_2O_8]$ (**2**), $(H_2DAP)[(UO_2)_2V_2O_8]$ (**3**), $(H_2PIP)[(UO_2)_2(VO_4)_2].0,8H_2O$ (**4**), $(H_2DMPIP)[(UO_2)_2V_2O_8]$ (**5**), $(H_2DABCO)[(UO_2)_2(VO_4)_2]$ (**6**) were prepared from mild-hydrothermal reactions using 1,2-ethylenediamine (EN); 1,3-diaminopropane (DAP); piperazine (PIP); 1-methylpiperazine (MPIP); 1,4-diazabicyclo[2,2,2]octane (DABCO). The structures of **1**, **4**, **5** and **6** were solved using single-crystal X-ray diffraction data while the structural models of **2** and **3** were established from powder X-ray diffraction data. In compounds **1**, **2**, **3** and **5**, the uranyl-vanadate layers are built from dimers of edge-shared UO_7 pentagonal bipyramids and dimers of edge-shared VO_5 square pyramids further connected through edge-sharing. In **1** and **3**, the layers are identical to that occurring in the carnotite group of uranyl-vanadates. In **2** and **5**, the V_2O_8 dimers differ in orientation leading to a new type of layer. The layers of compound **4** and **6** are built from chains of edge-shared UO_7 pentagonal bipyramids connected by VO_4 tetrahedra and are of uranophane-type anion topology. For the six compounds, the ammonium or organoammonium cation resides in the space between the inorganic layers. Crystallographic data: **1** monoclinic, space group $P2_1/c$ with $a = 6.894(2)$, $b = 8.384(3)$, $c = 10.473(4)$ Å and $\beta = 106.066(5)°$, **2** monoclinic, space group $P2_1/a$ with $a = 13.9816(6)$, $b = 8.6165(3)$, $c = 10.4237(3)$ Å and $\gamma = 93.125(3)°$, **3** orthorhombic, space group $Pmcn$ with $a = 14.7363(8)$, $b = 8.6379(4)$ and $c = 10.4385(4)$ Å, **4** monoclinic, space group $C2/m$ with $a = 15.619(2)$, $b = 7.1802(8)$, $c = 6.9157(8)$ Å and $\beta = 101.500(2)°$, **5** monoclinic, space group $P2_1/b$ with $a = 9.315(2)$, $b = 8.617(2)$, $c = 10.5246(2)$ Å and $\gamma = 114.776(2)°$, **6** monoclinic, space group $C2/m$ with $a = 17.440(2)$, $b = 7.1904(9)$, $c = 6.8990(8)$ Å and $\beta = 98.196(2)°$.
© 2006 Elsevier Inc. All rights reserved.

Keywords: Diamine uranyl vanadates; Crystal structure; Hydrothermal synthesis; Layered structure

1. Introduction

The solid state chemistry of uranyl-containing inorganic compounds is very rich in diversity. In particular, the association of hexavalent uranium polyhedra and oxoanions such as silicate, phosphate, vanadate, molybdate, tungstate, etc. constitutes a true building set leading to structures with varied architectures and dimensionalities. The basic building units are the uranium polyhedron, which can be hexagonal bipyramid, pentagonal bipyramid or distorted octahedron and the oxoanion polyhedron which can be tetrahedron, square or trigonal bipyramid or

octahedron. Many factors, such as U/oxoanion ratio, influence the degree of polymerisation between the uranium polyhedra, which can be connected directly by sharing equatorial oxygen atoms or through the oxoanions polyhedra. Due to the presence of uranyl bonds, which preclude the connections in a third dimension, there is a tendency to form layered structure in both mineral phases and synthetic compounds.

Our group of research mainly focuses on the solid state chemistry of uranyl-vanadates compounds [1–7]. In almost the studied oxides, the association of uranyl polyhedra through vanadate oxoanions leads to bi-dimensional anionic sheets with countercations lying in the interlayer space. However, in a recent paper, we described a novel three-dimensional (3D) uranyl-vanadate with an

*Corresponding author. Fax: +33 3 20 43 68 14.
E-mail address: Murielle.rivenet@ensc-lille.fr (M. Rivenet).

open-framework structure, which was obtained using small monovalent ions [8].

Owing to the potential applications of such type of materials (radioactive waste management, uranium geochemistry, ion-exchange and catalysis), a series of reactions was conducted in order to obtain novel layered and microporous uranium-bearing materials. An attempt to exert influence over structural features through the introduction of templating agents was undertaken. As amines have historically been used as charge balancing, space filling and templating agents in various uranium-based systems including molybdate [9–13], phosphate [14–18], phosphite [19], selenate [20], selenite [21], arsenate [17] sulphate [22–31] and fluoride [18,31–39], the investigations were carried out on the unexplored amine-uranyl-vanadates systems.

The new materials described in the present paper were obtained by reacting inorganic species (U/V ratio = 1) with an excess of amine by means of hydrothermal syntheses. Two linear diamines of different length (1,2-ethylenediamine (EN), 1,3-diaminopropane (DAP)) and three cyclic diamines based upon piperazine (PIP), 1-methylpiperazine (MPIP) and 1,4-diazabicyclo[2,2,2]octane (DABCO)) were used so as to vary the structure of the organic template. Syntheses led to six new layered uranyl-vanadates. Their crystal structure and thermal behaviour are reported hereafter.

2. Experimental

2.1. Synthesis

Uranyl nitrate ($UO_2(NO_3)_2 \cdot 6H_2O$—Prolabo, R.P. normapur), vanadium oxide (V_2O_5—Merck, Extra pur), concentrated chlorydric acid (Carlo Erba, 37%, $d = 1.186$) and amines (listed in Table 1) were used as received. For each synthesis, the solutions were heated to 180 °C, in 23 mL Teflon-lined steel autoclave Parr, for a time varying from 1 to 30 days. The resulting powders were collected after cooling to ambient temperature, filtration

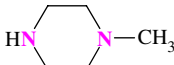and washing with desionised water. Reaction yields were not quantitatively determined.

$(NH_4)_2[(UO_2)_2V_2O_8]$ (1) was synthesised using $UO_2(NO_3)_2 \cdot 6H_2O \cdot (301.3 \text{ mg}, 0.600 \text{ mmol})$, V_2O_5 (54.6 mg, 0.300 mmol), EN ($C_2H_8N_2$—90.2 mg, 1.5 mmol) and desionised water (15.1 g, 840 mmol). The mixture was heated at 180 °C, for 30 days. Absence of ammonium in the starting reactants indicates that the formation of ammonium ions must involve the in situ decomposition of ethylenediamine. Amines decomposition under hydrothermal conditions has previously been observed using pyridine [40], imidazole [41], and guanidinium amines [42–45]. It is worth noting that we were enable to obtain $(NH_4)_2[(UO_2)_2V_2O_8]$ using a more direct source of ammonium cations.

$(H_2EN)[(UO_2)_2V_2O_8]$ (2) was prepared by hydrothermal reaction using a mixture of $UO_2(NO_3)_2 \cdot 6H_2O$ (301.3 mg, 0.600 mmol), V_2O_5 (54.6 mg, 0.300 mmol), EN ($C_2H_8N_2$—90.2 mg, 1.5 mmol) and desionised water (15.1 g, 840 mmol) added with chlorydric acid (HCl—109.4 mg, 3 mmol). Time of synthesis was limited to 1 day in order to avoid the ethylenediamine decomposition.

$(H_2DAP)[(UO_2)_2V_2O_8]$ (3), $(H_2PIP)[(UO_2)_2(VO_4)_2] \cdot 0.8H_2O$ (4), $(H_2DMPIP)[(UO_2)_2V_2O_8]$ (5) and $(H_2DABCO)[(UO_2)_2(VO_4)_2]$ (6) were obtained by conducting hydrothermal reactions at 180 °C, for 2 days, using a mixture of $UO_2(NO_3)_2 \cdot 6H_2O$ (301.3 mg, 0.600 mmol), V_2O_5 (54.6 mg, 0.300 mmol), HCl (109.4 mg, 3 mmol), desionised water (15.1 g, 840 mmol) and $C_3H_{10}N_2$ (111.2 mg, 1.5 mmol), $C_4H_{10}N_2$ (129.2 mg, 1.5 mmol), $C_5H_{12}N_2$ (150.3 mg, 1.5 mmol) and $C_6H_{12}N_2$ (168.3 mg, 1.5 mmol), respectively. During the synthesis of 5, some MPIP dismuted in 1,4-dimethylpiperazine (DMPIP) and PIP. The single crystals grew from MDPIP whereas the presence of PIP in the remaining solution was unambiguously evidenced by means of ^{13}C RMN.

Purity of the compounds was checked using X-ray powder diffraction. The X-ray powder patterns of the bulk samples can be fully indexed on the basis of the theoretical data calculated from the crystal structure results, which evidences that pure phases are obtained.

Table 1
Amine molecules of the studied UO_3–V_2O_5–amine systems

Name	Formula	Origin	Compound
1,2-Ethylenediamine (EN)	$H_2N(CH_2)_2NH_2$	ACROS, 99%, $d = 0.899$	**1** and **2**
1,3-Diaminopropane (DAP)	$H_2N(CH_2)_3NH_2$	ACROS, 99%, $d = 0.870$	**3**
Piperazine (PIP)		ACROS, 99%	**4**
1-Methylpiperazine (MPIP)		ACROS, 99%	**5**
1,4-Diazabicyclo[2,2,2]octane (DABCO)		ACROS, 97%	**6**

Presence of amine in the amine containing compounds **2–6** was confirmed using infra-red spectroscopy. The IR spectra showed that the bending vibrations of N–H are observed at around $1600\,cm^{-1}$ while the stretching vibrations of C–N, C–H and N–H are found in the 1020–1380, 2800–3000 and $3100–3570\,cm^{-1}$ regions. The bending vibrations of C–H are observed around $1500\,cm^{-1}$ for linear diamines containing compounds (**2** and **3**) and within the range $1410–1470\,cm^{-1}$ for cyclic diamines containing compounds (**4–6**).

2.2. Crystal structure determination

For compounds **1**, **4**, **5** and **6**, good quality single crystals for X-ray diffraction experiments were isolated under optical microscope. The selected crystals were mounted on a glass fibber and aligned on a Bruker SMART CCD X-ray diffractometer. Intensities were collected at room temperature using MoKα ($\lambda = 0.71073\,\text{Å}$) radiation selected by a graphite monochromator. The individual frames were measured using a ω-scan technique. Omega rotation and acquisition time were fixed at $0.3°$ and 20 s/

frame, respectively. About 1800 frames were collected in order to cover the full sphere. The Bruker programme SAINT [46] was used for intensity data integration and correction for Lorentz, polarisation and background effects. After data processing, absorption corrections were performed using a semi-empirical method based on redundancy with the SADABS programme [47]. Details of the data collection and refinement are given in Table 2.

The crystal structures were determined in the centrosymmetric space groups $P2_1/c$ for **1**, $P2_1/b$ for **5** and $C2/m$ for both **4** and **6**. A non-conventional setting was chosen for **5** in order to allow the description of the layers in the (100) plane for compounds **1**, **2**, **3** and **5**. The heavy atoms (U, V) positions were established by direct methods using SIR97 programme [48]. The oxygen, nitrogen and carbon atoms were localised from difference Fourier maps. The last cycles of refinement included atomic positions and anisotropic displacement parameters ADP for all atoms, excepted for partially occupied sites. Full-matrix least-squares structure refinements against F were carried out using the JANA2000 programme [49]. The atomic positional parameters and displacement parameters are given in

Table 2
Crystal data, intensity collection and structure refinement parameters for $(NH_4)_2[(UO_2)_2V_2O_8]$ (**1**), $(H_2PIP)[(UO_2)_2(VO_4)_2]\cdot0,8H_2O$ (**4**), $(H_2DMPIP)[(UO_2)_2V_2O_8]$ (**5**) and $(H_2DABCO)[(UO_2)_2(VO_4)_2]$ (**6**)

Compound	1	4	5	6
Chemical formula	$(NH_4)_2[(UO_2)_2V_2O_8]$	$(H_2PIP)[(UO_2)_2(VO_4)_2]\cdot0,8H_2O$	$(H_2DMPIP)[(UO_2)_2V_2O_8]$	$(H_2DABCO)[(UO_2)_2(VO_4)_2]$
Crystallographic data				
Formula weight (g/mol)	806	872.5	886.1	884.1
Crystal system	Monoclinic	Monoclinic	Monoclinic	Monoclinic
Space group	$P2_1/c$	$C2/m$	$P2_1/b$	$C2/m$
Unit-cell dimensions (Å)	$a = 6.894(2)$	$a = 15.619(2)$	$a = 9.315(2)$	$a = 17.440(2)$
	$b = 8.384(3)$	$b = 7.1802(8)$	$b = 8.617(2)$	$b = 7.1904(9)$
	$c = 10.473(4)$	$c = 6.9157(8)$	$c = 10.5246(2)$	$c = 6.8990(8)$
	$\beta = 106.066(5)$	$\beta = 101.500(2)$	$\gamma = 114.776(2)$	$\beta = 98.196(2)$
Cell volume (Å³)	581.7(4)	760.0(2)	767.0(2)	856.3(2)
Z	2	2	2	2
Density, calculated (g/cm³)	4.600(3)	3.814(1)	3.838(1)	3.4279(7)
F(000)	696	768	784	780
Intensity collection				
Wavelength (Å)	0.71069 (MoKα)	0.71069 (MoKα)	0.71069 (MoKα)	0.71069 (MoKα)
θ range (deg)	3.07–28.67	3.01–23.27	2.41–27.95	2.98–28.33
Data collected	$-9 \leqslant h \leqslant 9$	$-17 \leqslant h \leqslant 17$	$-12 \leqslant h \leqslant 12$	$-23 \leqslant h \leqslant 23$
	$-11 \leqslant k \leqslant 11$	$-7 \leqslant k \leqslant 7$	$-13 \leqslant k \leqslant 13$	$-9 \leqslant k \leqslant 9$
	$-13 \leqslant l \leqslant 13$	$-7 \leqslant l \leqslant 7$	$-10 \leqslant l \leqslant 10$	$-9 \leqslant l \leqslant 9$
No. of reflections measured	4549	2005	5425	3549
No. of independent reflections	1364	590	1633	1105
Redundancy	3.335	3.40	3.32	3.212
No. of unique reflections ($I > 3\sigma(I)$)	1186	530	1250	1027
μ (MoKα) (mm^{-1})	29.37	22.50	22.30	19.97
T_{min}/T_{max}	0.466	0.367	0.680	0.202
$R(F^2)_{int}$	0.0397	0.0313	0.0492	0.0319
Refinement				
No. of parameters	83	62	110	77
Weighting scheme	$1/\sigma^2$	$1/\sigma^2$	$1/\sigma^2$	$1/\sigma^2$
$R(F)$ obs/all	0.0276/0.0340	0.0214/0.0240	0.0332/0.0502	0.0238/0.0250
$wR(F)$ obs/all	0.0296/0.0304	0.0244/0.0249	0.0291/0.0306	0.0300/0.0302
Max, min $\Delta\rho$(e/Å³)	1.97/-1.84	0.78/-1.01	2.32/-1.57	1.89/-1.20

Table 3—compound **1**, Table 4—compound **5** and Table 5—compounds **4** and **6**. Some selected interatomic distances are reported in Table 6—compounds **1** and **5**, and Table 7—compounds **4** and **6**.

As no suitable crystals could be found for the (H$_2$EN)[(UO$_2$)$_2$V$_2$O$_8$] (**2**) and (H$_2$DAP)[(UO$_2$)$_2$V$_2$O$_8$] (**3**) samples, their crystal structure models were checked using X-ray powder diffraction data. The data were collected by means of a Huber G670 diffractometer using an asymmetric Guinier flat sample transmission geometry, equipped with a 2D detector (Image Plate) covering the 2θ range [6–100°]. The **2** and **3** samples were exposed, respectively, for 1 h and half an hour to a monochromatized Cu$K\alpha_1$ radiation obtained with a Germanium Johanson monochromator. The structural models containing only the uranium–vanadium–oxygen sheets led to the results reported in Table 8.

For **2**, the **b** and **c** parameters correspond to a carnotite-type layer, however the space group symmetry operations are incompatible with such a structure. As we could not find any structurally related compound, we attempted to solve the structure by ab initio procedures. The pattern decomposition option of the JANA2000 package [49] was used to extract corrected structure factors from a limited

Table 3
Atomic coordinates and isotropic displacement parameters (in Å^2) for (NH$_4$)$_2$[(UO$_2$)$_2$V$_2$O$_8$] (**1**)

Atom	Wyck.	x	y	z	U_{eq}
U1	4e	0.01539(4)	0.47727(3)	0.81974(2)	0.0110(2)
V1	4e	0.1147(2)	0.8516(2)	0.0557(2)	0.0122(4)
O1	4e	0.2776(8)	0.4265(7)	0.8795(5)	0.020(2)
O2	4e	−0.2457(9)	0.5260(6)	0.7598(5)	0.019(2)
O3	4e	0.0406(8)	0.0607(6)	0.1079(5)	0.016(2)
O4	4e	0.0418(8)	0.6553(6)	−0.0044(4)	0.016(2)
O5	4e	0.3484(9)	0.8708(7)	0.0648(5)	0.025(2)
O6	4e	0.0930(8)	0.7909(6)	0.2192(5)	0.016(2)
N1	4e	−0.458(2)	0.7697(9)	0.8626(7)	0.029(3)

Table 4
Atomic coordinates and isotropic displacement parameters (in Å^2) for (H$_2$DMPIP)[(UO$_2$)$_2$V$_2$O$_8$] (**5**)

Atom	Wyck.	x	y	z	U_{eq}
U1	4e	0.48421(4)	0.47738(4)	−0.31760(3)	0.0125(2)
V1	4e	0.4327(2)	0.1248(2)	−0.4674(2)	0.0149(7)
O1	4e	0.6969(8)	0.5718(8)	−0.3076(7)	0.024(3)
O2	4e	0.2702(7)	0.3856(8)	−0.3308(7)	0.020(3)
O3	4e	0.5371(8)	0.0699(8)	−0.5981(6)	0.017(3)
O4	4e	0.5028(8)	0.3475(8)	−0.5114(6)	0.016(3)
O5	4e	0.2473(7)	0.0417(8)	−0.4949(7)	0.022(3)
O6	4e	0.4657(8)	0.1971(7)	−0.2998(6)	0.019(3)
N1	4e	0.004(2)	0.488(2)	−0.3662(9)	0.061(6)
C1	4e	0.095(2)	0.648(2)	−0.424(2)	0.041(5)
C2	4e	−0.113(2)	0.350(2)	−0.436(2)	0.043(5)
C3	4e	−0.015(2)	0.487(2)	−0.222(2)	0.062(8)

Table 5
Atomic coordinates and isotropic displacement parameters (in Å^2) for (H$_2$PIP)[(UO$_2$)$_2$(VO$_4$)$_2$]·0.8H$_2$O (**4**) (**bold type**) and (H$_2$DABCO)[(UO$_2$)$_2$(VO$_4$)$_2$] (**6**) (*italic type*)

Atom	Site	Occ.	x	y	z	$U_{eq/iso}$*
I. [(UO$_2$)$_2$(VO$_4$)$_2$] layer						
U1	**4i**		**0.75640(3)**	**0**	**−0.11646(6)**	**0.0118(2)**
	4i		*0.75602(2)*	*0*	*−0.11813(3)*	*0.0138(2)*
V1	**4i**		**0.7204(2)**	**0**	**−0.6690(2)**	**0.0108(6)**
	4i		*0.71988(7)*	*0*	*−0.6700(2)*	*0.0138(3)*
O1	**4i**		**0.8722(5)**	**0**	**−0.036(1)**	**0.020(3)**
	4i		*0.8588(3)*	*0*	*−0.0535(8)*	*0.027(2)*
O2	**4i**		**0.6409(5)**	**0**	**−0.191(2)**	**0.026(3)**
	4i		*0.6528(3)*	*0*	*−0.1811(8)*	*0.027(2)*
O3	**4i**		**0.7838(5)**	**0**	**−0.435(1)**	**0.020(3)**
	4i		*0.7763(3)*	*0*	*−0.4412(7)*	*0.020(2)*
O4	**8j**		**0.7433(4)**	**−0.1807(7)**	**−0.8236(7)**	**0.021(2)**
	8j		*0.7428(2)*	*−0.1799(5)*	*−0.8221(5)*	*0.024(2)*
O5	**4i**		**0.6179(6)**	**0**	**−0.659(2)**	**0.032(3)**
	4i		*0.6289(4)*	*0*	*−0.6494(9)*	*0.038(2)*
II. Organic entity and water molecule in 4						
N1	**8j**	**0.5**	**0.504(2)**	**−0.386(2)**	**−0.673(2)**	**0.025(4)***
C1	**8j**	**0.5**	**0.532(2)**	**−0.432(2)**	**−0.673(2)**	**0.022(5)***
C2	**8j**	**0.5**	**0.482(2)**	**−0.304(2)**	**−0.543(2)**	**0.026(5)***
O6w	**4g***	**0.42(2)**	**0.5**	**−0.184(2)**	**0**	**0.014(6)***
N1	*8j*	*0.5*	*0.0660(5)*	*−0.037(2)*	*0.453(2)*	*0.033(3)* *
C1	*8j*	*0.5*	*0.9325(9)*	*0.153(3)*	*0.371(2)*	*0.059(7)*
C2	*8j*	*0.5*	*0.0182(8)*	*0.118(2)*	*0.296(3)*	*0.068(7)*
C3	*8j*	*0.25*	*0.040(2)*	*0.163(4)*	*0.447(6)*	*0.054(9)* *
C4	*8j*	*0.25*	*0.946(2)*	*0.154(5)*	*0.451(7)*	*0.047(9)* *

Table 6
Principal interatomic distances (Å) for **1** and **5**

Compound **1**		Compound **5**	
U1–O1	1.793(5)	U1–O1	1.802(7)
U1–O2	1.782(6)	U1–O2	1.816(6)
U1–O3[iv]	2.295(6)	U1–O3[i]	2.340(6)
U1–O4[i]	2.338(5)	U1–O4	2.368(7)
U1–O4[ii]	2.356(5)	U1–O4[iii]	2.319(7)
U1–O6[i]	2.369(5)	U1–O6	2.356(7)
U1–O6[iii]	2.342(5)	U1–O6[ii]	2.327(7)
V1–O3[v]	1.946(5)	V1–O3	1.857(8)
V1–O3[v]	1.899(5)	V1–O3[iv]	1.940(8)
V1–O4	1.784(5)	V1–O4	1.809(7)
V1–O5	1.596(6)	V1–O5	1.594(6)
V1–O6	1.832(6)	V1–O6	1.853(6)
		V1–V1[iv]	2.988(3)
		N1–O2	2.98(2)
		N1–C1	1.42(2)
		N1–C2	1.43(2)
		N1–C3	1.53(2)
		C1–C2[vi]	1.48(2)

Symmetry codes for **1** (i) −x, −y, 1−z; (ii) −x, 1−y, 1−z; (iii) x, 3/2−y, 1/2+z; (iv) x, 1/2−y, 1/2+z; (v) −x, 1−y, −z; (vi) −1+x, 1/2−y, 3/2+z; (vii) −1−x, −y, 1−z; for **5** (i) 1−x, 1/2−y, 1/2+z; (ii) x,1/2+y, −1/2−z; (iii) 1−x, 1−y, −1−z; (iv) 1−x, −y, −1−z; (v) 1−x, 1/2−y, −1/2+z; (vi) −x,1−y, −1−z.

Table 7
Principal interatomic distances (Å) for **4** and **6**

Compound **4**		Compound **6**	
U1–O1	1.775(8)	U1–O1	1.784(5)
U1–O2	1.783(8)	U1–O2	1.791(5)
U1–O3	2.326(7)	U1–O3	2.306(5)
U1–O4[i]	2.448(5)	U1–O4[i]	2.456(4)
U1–O4[ii]	2.330(5)	U1–O4[ii]	2.339(4)
U1–O4[iii]	2.330(5)	U1–O4[iii]	2.339(4)
U1–O4[iv]	2.448(5)	U1–O4[iv]	2.456(4)
V1–O3	1.721(7)	V1–O3	1.737(5)
V1–O4	1.763(5)	V1–O4	1.747(4)
V1–O4[v]	1.763(5)	V1–O4[v]	1.747(4)
V1–O5	1.62(1)	V1–O5	1.613(7)
C1–C2	1.59(2)	C1–C2[vii]	1.67(2)
		C3–C4[xiv]	1.64(5)
N1[xiv]–C1	1.38(2)	N1[xii]–C1	1.47(2)
N1[xii]–C2	1.54(2)	N1[v]–C2	1.40(2)
		N1–C3	1.51(3)
		N1–C4[x]	1.55(4)
N1[i]–O6w	2.71(2)	N1[vii]–O3	2.78(1)
N1[xii]–O6w	2.71(2)	N1[viii]–O3	2.78(1)

Symmetry codes (i) $-x, -y, 1-z$; (ii) $3/2-x, -1/2-y, -1-z$; (iii) $3/2+x$, $1/2-y, -1+z$; (iv) $1/2+x, 1/2-y, 1+z$; (v) $1/2+x, 1/2-y,z$; (vi) $3/2-x$, $-1/2-y, -2-z$; (vii) $1-x, -y, -z$; (viii) $1+x, -y, z$; (ix) $2+x, -y, 1+z$; (x) $1+x, -y, 1+z$ (xi) $3/2+x, 1/2-y,z$; (xii) $1-x, -y, 1-z$; (xiii) $x, -y$, $1+z$; (xiv) $-1-x, -y, -z$; (xv) $-1/2+x, 1/2-y, z$; (xvi) $2-x, -y, 1-z$.

Table 8
Structure refinement parameters for $(H_2EN)[(UO_2)_2V_2O_8]$ (**2**) and $(H_2DAP)[(UO_2)_2V_2O_8]$ (**3**)

Compound no.	2	3
Chemical formula	$(H_2EN)[(UO_2)_2V_2O_8]$	$(H_2DAP)[(UO_2)_2V_2O_8]$
Crystallographic data		
Formula weight (g/mol)	832	846.1
Crystal system	monoclinic	orthorhombic
Space group	$P2_1/a$	$Pmcn$
Unit-cell dimensions (Å)	$a = 13.9816(6)$	$a = 14.7363(8)$
	$b = 8.6165(3)$	$b = 8.6379(4)$
	$c = 10.4237(3)$	$c = 10.4385(4)$
	$\gamma = 93.125(3)$	
Cell volume (Å^3)	1253.91(9)	1327.5(2)
Z	4	4
Density, calculated (g/cm^3)	4.406	4.232
Refinement		
R_p/Rw_p	0.0133/0.0180	0.0168/0.0258
R_{obs}/Rw_{obs}	0.0634/0.0573	0.0811/0.0815
R_{all}/Rw_{all}	0.0679/0.0579	0.0959/0.0850
R_{exp}	0.0341	0.0382

error, peak shape (pseudo-Voigt). The refinement converged to $Rw_p = 1.29$ and $R_p = 0.99\%$. A total of 363 reflections were used as input to the direct-methods SIR97 programme [48]. The positions of two U atoms were derived from this method. At this stage, the positions of the V atoms were deduced from a difference-Fourier map. Then, after refining the heavy atoms position and ADP, another difference-Fourier map revealed O atoms. At this stage we used soft constraints in the U–O and V–O bonds to avoid the structure blow up and to keep a reasonable geometry for the anionic sheet. Unfortunately, probably due to the high contrast between the U and (C–N–H) atoms of the amines, we were not able to see these last types of atomic species in a last difference-Fourier map. Without these "light" atoms and refining all positional parameters R_{wp} dropped to 1.80% (Table 8). Refining isotropic temperature factors freely resulted in some negative values. It is well known that temperature factors, for complex structures with heavy cations and medium resolution X-ray powder data, are quite unreliable. Hence, we decided to refine an overall isotropic temperature factor for U and V atoms and to fix an overall temperature factor for the oxygen atoms. The plot of observed and calculated patterns is represented Fig. 1. It shows the very good agreement between the experimental and calculated data. The refined positional parameters are reported in Table 9.

For compound **3**, the values of the cell parameters and the XRD pattern are very similar to those of uranyl vanadates of divalent A cations built from carnotite type layers. The space group deduced from the X-ray powder pattern indexation, *Pmcn*, is adopted for $A =$ Ca [50], Mn, Co [51], Ni, Cd, Zn [52]. The precise lattice parameters were obtained from profile matching and, using the structural model of the divalent carnotite-type compounds layers. The reliability factors reported in Table 8 were obtained.

2.3. High-temperature X-ray diffraction

The high-temperature X-ray powder diffraction patterns were recorded using a Guinier–Lenné moving film camera. The samples were deposited on the sample holder (gold grid) using an ethanol slurry which yields, upon evaporation, a regular layer of powdered compound. The high-temperature X-ray diffraction patterns were recorded in the temperature range from 20 to 600 °C with a heating rate in the range [12–15° h^{-1}].

2.4. Thermal analysis

The thermal analyses were performed on a Setaram coupled TGA-DTA 2-16.18 apparatus. Analyses were undertaken in air, in the temperature range from 20 to 600 °C, with a heating rate of 300° h^{-1}, in platinum crucibles.
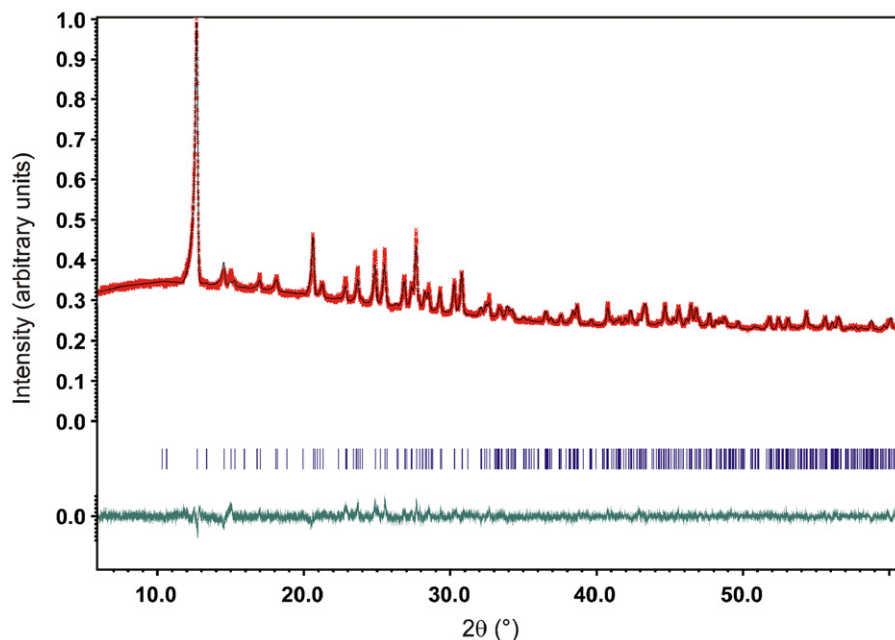
region of the diffractogram ($6 < 2\theta < 60°$). The pattern was fit without any structural model by refining the overall parameters: background, unit-cell parameters, zero-point

Fig. 1. Observed, calculated XRD patterns and their difference for $(H_2EN)[(UO_2)_2V_2O_8]$ (compound **2**).

Table 9
Atomic coordinates and isotropic displacement parameters (in Å^2) for $(H_2EN)[(UO_2)_2V_2O_8]$ (**2**)

Atom	Wyck.	x	y	z	$U_{iso/eq}$
U1	4e	0.2367(4)	−0.2646(9)	0.2617(3)	0.009(2)
U2	4e	0.2576(5)	−0.236(1)	0.6282(3)	0.009(2)
V1	4e	0.276(2)	0.107(2)	0.470(2)	0.009(2)
V2	4e	0.679(2)	0.386(3)	0.092(2)	0.009(2)
O1	4e	0.3849(6)	−0.232(3)	0.608(3)	0.006
O2	4e	0.1306(4)	−0.242(1)	0.650(2)	0.006
O3	4e	0.3649(3)	−0.259(3)	0.257(4)	0.006
O4	4e	0.1086(4)	−0.2723(9)	0.265(2)	0.006
O5	4e	0.241(2)	−0.0941(9)	0.4378(3)	0.006
O6	4e	0.387(2)	0.144(6)	0.441(5)	0.006
O7	4e	0.738(2)	0.5924(9)	0.0464(3)	0.006
O8	4e	0.570(2)	0.402(5)	0.053(5)	0.006
O9	4e	0.2202(8)	0.198(7)	0.3497(9)	0.006
O10	4e	0.7336(3)	0.463(1)	0.248(2)	0.006
O11	4e	0.267(2)	0.321(5)	0.5411(9)	0.006
O12	4e	0.2627(5)	0.036(2)	0.638(2)	0.006

3. Results

3.1. Cation coordination polyhedra

For all the studied compounds, each uranium atom is strongly bonded to two oxygen atoms forming a nearly linear uranyl cation $(UO_2)^{2+}$ with an O–U–O bond angle ranging from 178.6(4) to 179.5(3)° and U–O bond lengths ranging from 1.775(8) to 1.816(6) Å (average value of 1.79(2) Å). These uranyl cations are coordinated by five oxygen atoms located in the equatorial plane which forms [UO_7] pentagonal bipyramids. The equatorial oxygen ligands show significant variations with U–O distances

ranging from 2.295(6) to 2.458(3) Å. However, the average value, 2.36(6) Å, is in good agreement with the average bond length of 2.37(9) Å calculated for uranyl polyhedra of numerous well-refined structures [53].

The vanadium atoms of structures **1**, **2**, **3** and **5** are pentacoordinated by five oxygen atoms in a square pyramidal arrangement. Two VO_5 square pyramids related by an inversion centre share an O–O edge to form a V_2O_8 dimeric unit. Within the VO_5 square pyramids, the apical V–O bond is shorter than the vanadium–oxygen distances of the square base. This vanadyl V–O bond distance is close to that calculated in various carnotite-type compounds [54] and V_2O_5 [55].

In $(H_2PIP)[(UO_2)_2(VO_4)_2] \cdot 0.8H_2O$ (**4**) and (H_2DABCO) $[(UO_2)_2(VO_4)_2]$ (**6**), the vanadium atoms occupy one crystallographic site with tetrahedral environment. The tetrahedra are slightly distorted with V–O distances in the range from 1.721(7) to 1.763(5) Å when the oxygen atoms are shared with a UO_7 polyhedron and shorter distances with O(5) atom not involved in uranium coordination, i.e., 1.62(1) and 1.611(6) Å for **4** and **6**, respectively.

Bond-valence sums were calculated using parameters given by Burns et al. [53] for U–O bonds and by Tytko et al. [56] for V–O bonds. Calculations resulted in values ranging from 6.00(2) to 6.19(3) v.u. for U^{6+} and from 5.08(5) to 5.14(4) v.u. for V^{5+} with oxygen valences ranging from 1.57(2) to 2.18(2) v.u. The lowest sums correspond to O atoms not shared between UO_7 and VO_4 or VO_5 polyhedra.

3.2. Structural connectivity

The structural building unit block, with labelled scheme, constituted from two edge-shared UO_7 pentagonal

bipyramids and two edge-shared VO_5 square pyramids is shown on Fig. 2 for compounds **1**, **2** and **5**.

Compound **1** is isotypic with the mineral carnotite $K_2[(UO_2)_2V_2O_8]$ and other $A_2[(UO_2)_2V_2O_8] \cdot nH_2O$ compounds where A is a monovalent ion [45], $CsUNbO_6$ [57] and $A_2[(UO_2)_2Cr_2O_8] \cdot nH_2O$ (A = K, Rb, Cs) [58]. The structural arrangement between the edge-shared dimers, V_2O_8, and the edge- and corner-shared pentagonal
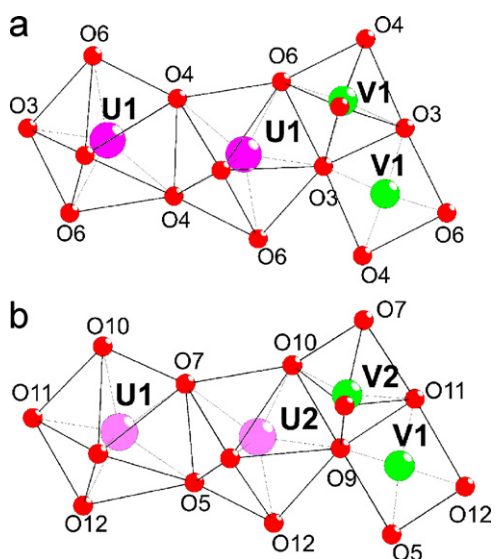

Fig. 2. The structure building unit block formed of two edge-shared UO_7 pentagonal bipyramids and two edge-shared VO_5 square pyramids further connected by edge with the labelled scheme for (a) compounds **1** and **5**, (b) compound **2**.

bipyramids, UO_7, further linked by edge-sharing, forms sheets of composition $[(UO_2)_2V_2O_8]^{2-}$ parallel to (100) (Fig. 3b). The ammonium anions are located in the interlayer space and insure the cohesion of the structure.

Compound **3** is built from the same layers. The layers packing along **a**-axis depends upon the interleaving cation. In **1**, as in almost all the monovalent containing $A_2[(UO_2)_2V_2O_8] \cdot xH_2O$ compounds, adjacent layers noted P are deduced by **a** translation, resulting in the simple PPPP sequence (Fig. 4a). In compound **3** there is a second layer, labelled b, image of P in a (100) mirror plane. P and b layers alternate to yield a PbPb sequence (Fig. 4b). Such a sequence was previously evidenced in $A[(UO_2)_2V_2O_8] \cdot xH_2O$ compounds containing a divalent A cation [50–52].

Using the description developed by Burns et al. [59], the francevillite anion topology of the $[(UO_2)_2V_2O_8]^{2-}$ sheets is represented in Fig. 3a. Compounds **2** and **5** are built from sheets with the same anion topology and with the same occupation of pentagons by U, squares by V and empty triangles (Fig. 3c). However, in contrast with the previous **1** and **3** compounds and with all the carnotite-type layer containing compounds described up today, half of the V_2O_8 units are reversed (Fig. 3c) compared to the P sheets (Fig. 3b). A V_2O_8 dimer can be referenced as *ud* with a tetragonal pyramid that point *up* and one *down*. In P layers the dimers alternate, along [010], to form the isomer *ud/du*. In opposite, the new anionic layer, labelled P' hereafter, represents the *du/du* geometrical isomer. In compound **5**, a layer b' is deduced from P' by a two-fold axis running along **c**-axis so as the stacking sequence is P'b'P'b' (Fig. 4d)
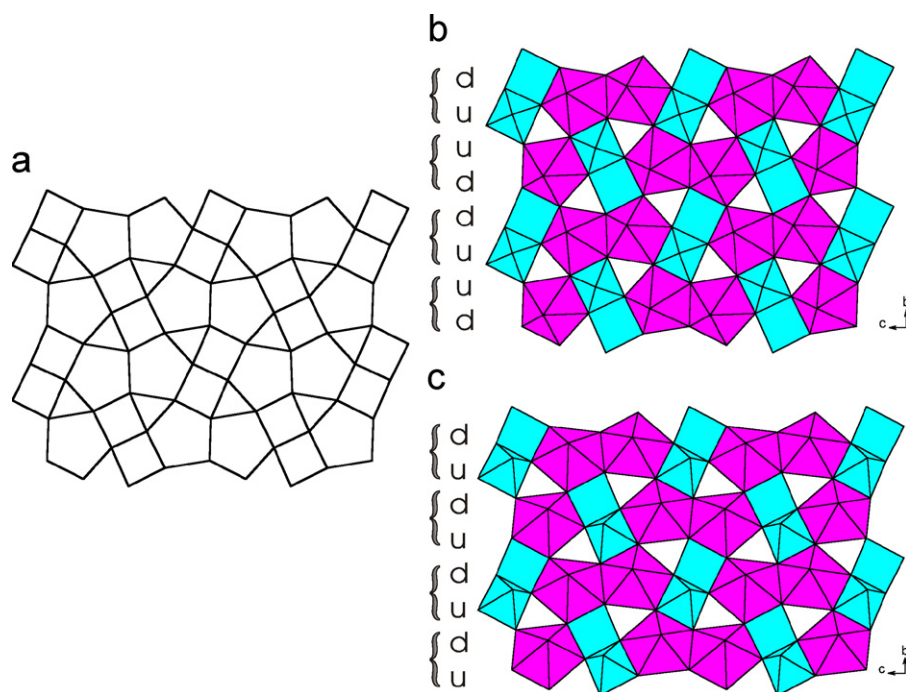

Fig. 3. The francevillite anion topology (a) and the uranyl vanadate layers in carnotite-type compounds: (b) *ud/du* isomer layers P in M^{+}-, M^{2+}- or 1, 3-diaminopropane-containing compounds; (c) *du/du* isomer layers P' in ethylenediamine- and 1,4-dimethylpiperazine-containing compounds.
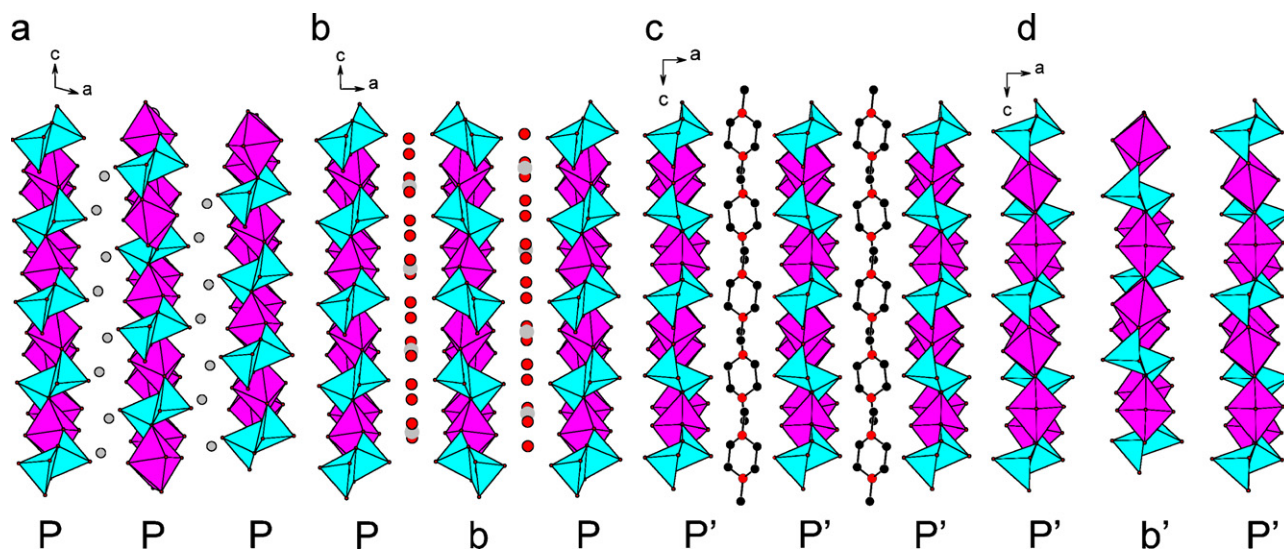
Fig. 4. Stacking of the P and P′ layers in carnotite type compounds containing monovalent ions and **1** (a), divalent inorganic ions and **3** (b), 1,4-dimethylpiperazine **5** (c) and ethylenediamine (not localised from X-ray powder diffraction data) **6** (d).

while the stacking sequence in structure **2** can be described as P′P′P′P′ (Fig. 4c).

Compounds **4** and **6** are isotypic and contain the same $[(UO_2)_2(VO_4)_2]^{2-}$ layer built from $(UO_5)_\infty$ zig-zag chains of edge shared UO_7 pentagonal bipyramids running down the ***b***-axis further connected by VO_4 tetrahedra. The uranyl vanadate layer has the uranophane sheets anion topology (Fig. 5) adopted by many mineral or synthetic inorganic or hybrid organic–inorganic uranyl compounds. In the two structures, all the tetrahedra that share edges with one side of a uranyl chain point down (*d*), and all the tetrahedra along the other side point up (*u*), which corresponds to the geometrical isomer *du/du* as defined by Locock et al. [60]. The 3D structure results from the alternate stacking of inorganic layers and sheets of protonated amines (and occluded water molecules in **4**).

It should be noticed that with triethylamine, Locock and Burns [17] obtained the same structural arrangement but with another geometrical isomer of the uranyl arseniate layer whereas with DABCO molecules an autunite-type uranyl arseniate layer is formed.

3.3. Interlayer space occupation

In order to study the role of amine on the structural arrangement of the uranyl-vanadates, the location and connectivity of amines in the interlayer space was systematically investigated for the single crystal studied compounds.

Projected along [100], the interleaving NH_4^+ cations in **1** appears at the centre of the inoccupied triangles of the francevillite anion-type topology (Fig. 6). The NH_4^+ ions occupy the same position than the alkali atoms in the $A_2[(UO_2)_2V_2O_8]$ compounds. Investigation of the N–O distances evidences eight N–O contacts in a continuous range from 2.8 to 3.3 Å without any O–N–O angle
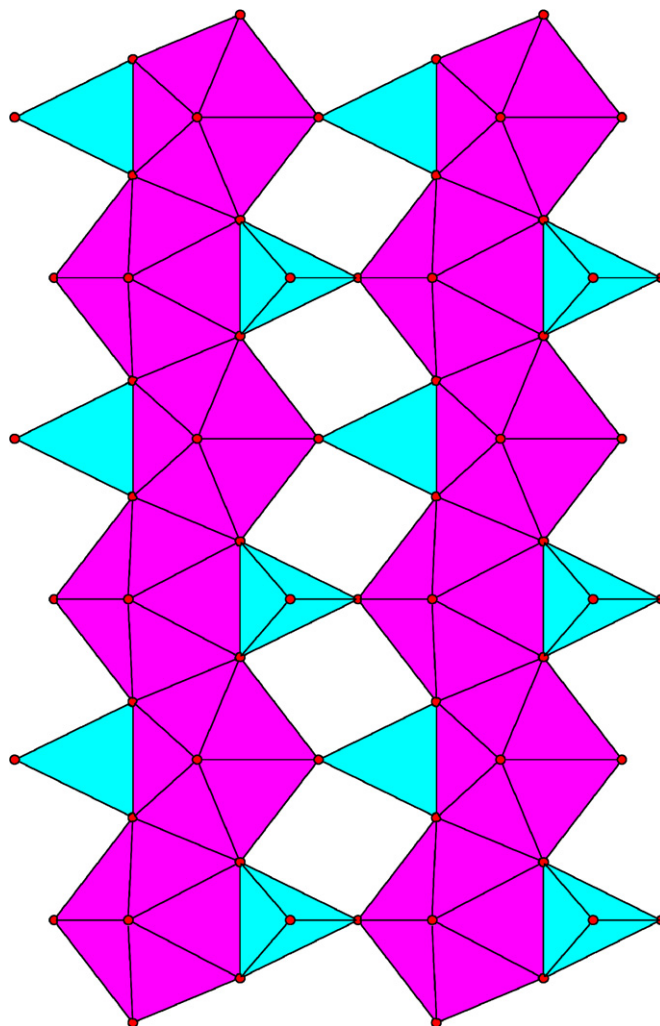

Fig. 5. The uranophane type uranyl vanadate sheet in the structure of **4** and **6**.
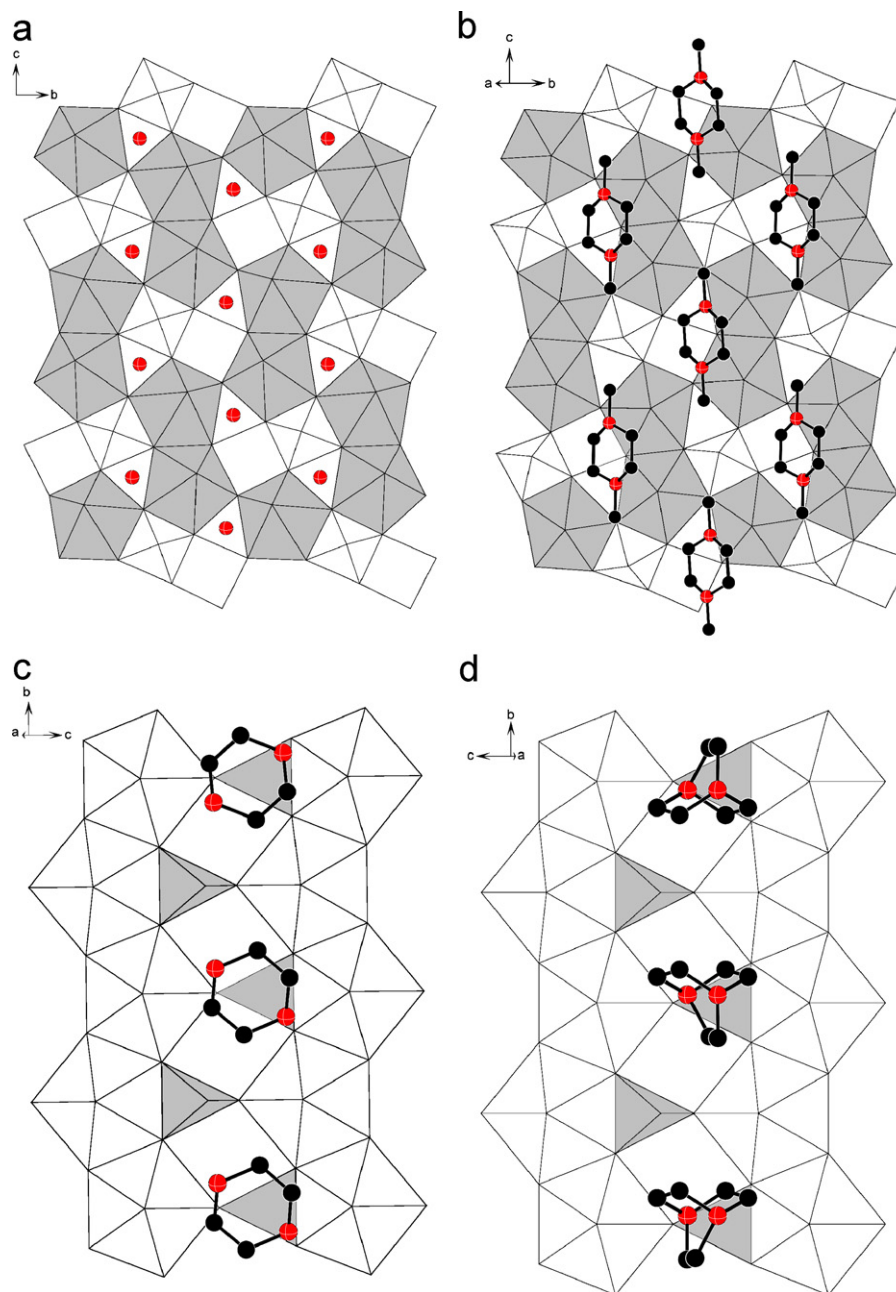
Fig. 6. Localisation of the ammonium cation above the *ud/du* geometrical isomer layer in **1** (a), dimethylpiperazine ions above the *du/du* geometrical isomer layer in **5** (b), piperazine and diazabicyclooctane above the uranophane-type layer in **4** and **6**, (c) and (d), respectively.

corresponding to a tetrahedral coordination involving hydrogen bonds, so the pseudo-alkali character of the ammonium cation dominates in this compound. Fig. 7 shows the variation of the inter-layer distance $a \sin \beta$ for the $A_2[(UO_2)_2V_2O_8]$ compounds versus the ionic radii of the 8-coordinated A^+ ions [61]. Using the value of ionic radius reported by Khan and Bauer [62] for the 8-coordinated NH_4^+ (1.66 Å), the corresponding point does not fit with this straightforward variation, so according to Shannon [61] for the 6-coordination, we should conclude that NH_4^+ is not different in size from Rb^+ for the 8-coordination.

Although in **2** and **3** the diprotonated amines could not be localised one can imagine that they separate the

inorganic layers from one another, creating spacing of approximately 6.98 and 7.37 Å between the uranium atom planes, and stabilise the structures, both through balancing the negative charge of the inorganic layer and donating hydrogen bonds.

In **5**, the $[H_2DMPIP]^{2+}$ cations, with a chair conformation, are aligned along [001] in the space between the $[(UO_2)_2V_2O_8]^{2-}$ layers. The mean plane of the diamines is inclined of about 45° from the layer. Comparison between Figs. 6a and b evidences that the arrangement of the diamines in the interlayer space is incompatible with the *ud/du* isomer. The two nitrogen atoms of the $[H_2DMPIP]^{2+}$ cation donate their hydrogen bonds to the

apical oxygen atoms O(2) of two parallel uranyl-vanadate layers with a N(1)–O(2) distance of 2.98(2) Å.

In **4** and **6**, the $[H_2PIP]^{2+}$ and $[H_2DABCO]^{2+}$ cations reside between the inorganic layers and are located above the VO_4 tetrahedra of the $[(UO_2)_2(VO_4)_2]^{2-}$ uranophane layers that points down. In **4**, the interleaving $[H_2PIP]^{2+}$ molecules lie almost parallel to (100) plane with no strong hydrogen bonds with the uranyl vanadate layer: instead, the shortest N–O distances, 2.71(2) Å, involve an oxygen of the interleaving water molecules. The $[H_2PIP]^{2+}$ molecules adopt a boat conformation which can be present in two possible orientations related by a mirror parallel to (001). Thus, the site occupancy factors for the C(1), C(2) and N(1) atoms, located in a general position, were fixed at 0.5. In **6**, the pseudo-trigonal $[H_2DABCO]^{2+}$ cations can be found with two possible orientations (Fig. 8) modelled by half occupying the general positions of C(1), C(2) and N(1) atoms. Moreover, a disorder presented by the C(3)–C(4) group, was taken in account by fixing at 0.25 the site occupancy for C(3) and C(4) atoms, located in a general position. The $[H_2DABCO]^{2+}$ molecule are slightly distorted with C(1)–C(2) and C(3)–C(4) bond lengths, respectively, equivalent to 1.67(2) and 1.64(5) Å and N(1)–C bond lengths varying within the range [1.40–1.55] Å. The cations are oriented such as their ammonium moities are directed toward the corner sharing

oxygen atoms O(3) of the VO_4–UO_7 units with a strong N–O(3) hydrogen bond of 2.78(1) Å lying along the N–N axis. That indicates the presence of a 3D hydrogen bonds network that constrains the $[H_2DABCO]^{2+}$ cations to lie almost perpendicular to the layers as previously observed in diamine templated uranium sulphates [26].

3.4. Thermal behaviour

For compound **1**, a one-step decomposition from $(NH_4)_2[(UO_2)_2V_2O_8]$ to $(UO_2)_2V_2O_7$ [63] corresponding to 6.1% weight loss in accordance with the 6.5% theoretical loss is observed between 375 and 470 °C on the TGA curve. The thermal behaviour is confirmed by high-temperature X-ray diffraction experiment.

For all the amine-bearing materials (**2–6**), the decomposition of the amine and the modification of the uranyl-vanadate arrangement occur in several steps between 280 and 550 °C. On the high-temperature X-ray diffraction patterns a non-crystalline zone is observed from approximately 290 to 440 °C between the starting uranyl-vanadate and the final product $(UO_2)_2V_2O_7$ [61]. The total weight losses are in agreement with the calculated values for the transformation from (DIAMINE)[uranyl-vanadate] to $(UO_2)_2V_2O_7$ (exp./theor. (%): 9.0/9.4–11.3/10.9–11.5/12.0–14.8/14.9–14.0/14.6 for compounds **2–6**, respectively).

4. Conclusion

For the five studied diamine-containing compounds, uranyl vanadates layers with formula $(UVO_6)^{2-}$ are formed. Two types of layers were obtained. For compounds **1**, **2**, **3** and **5**, the $[(UO_2)_2V_2O_8]^{2-}$ layers are similar to that of the mineral carnotite with two geometrical isomers distinguished by the orientations of the V_2O_8 units. For the two other compounds, the uranophane-type layers are built from chains of edge-shared UO_7 pentagonal bipyramids connected through VO_4 tetrahedra. In all the compounds, the diprotonated amines reside between the inorganic layers, balancing charge and often donating hydrogen bonds to the layers. However, as previously noted by Almond and Albrecht-Schmitt [21], it is difficult
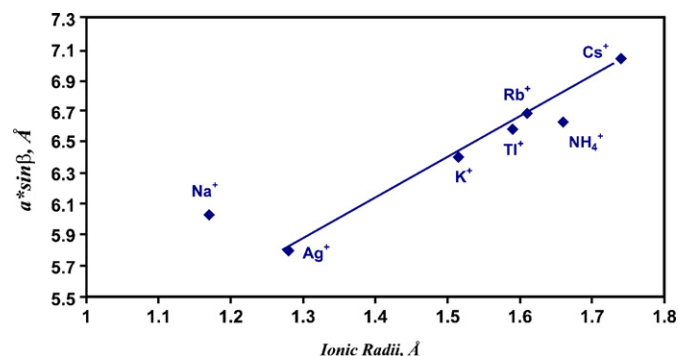

Fig. 7. Variation of the interlayer distance versus the ionic radii of 8-coordinated monovalent ion in $A_2[(UO_2)_2V_2O_8]$ compounds built on carnotite-type layers.
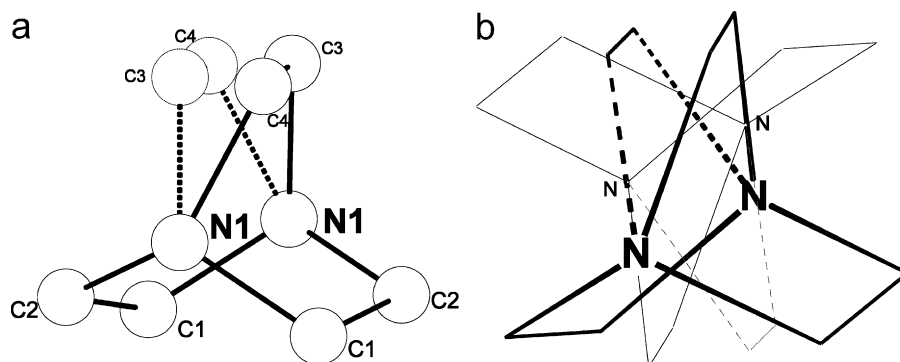

Fig. 8. One orientation of the pseudo-trigonal $[H_2DABCO]^{2+}$ cations showing the disorder presented by the C(3)–C(4) group. The general positions of C(1), C(2) and N(1) atoms are half occupied (a). Scheme of the two orientations adopted by the $[H_2DABCO]^{2+}$ cations (b).

to prove the template role of the organoammonium cations which sometimes act only as charge balancing and space filling when they are used as countercation in hydrothermal syntheses.

For all compounds, thermal decomposition led to the divanadate $(UO_2)_2V_2O_7$. Further experiments using other amines to built 3D uranyl-vanadate frameworks are in progress.

Acknowledgments

References

[1] I. Duribreux, C. Dion, M. Saadi, F. Abraham, J. Solid State Chem. 146 (1999) 258.

[2] C. Dion, S. Obbade, E. Raekelboom, M. Saadi, F. Abraham, J. Solid State Chem. 155 (2000) 342.

[3] M. Saadi, C. Dion, F. Abraham, J. Solid State Chem. 150 (2000) 72.

[4] S. Obbade, C. Dion, L. Duvieubourg, M. Saadi, F. Abraham, J. Solid State Chem. 173 (2003) 1.

[5] I. Duribreux, M. Saadi, S. Obbade, C. Dion, F. Abraham, J. Solid State Chem. 172 (2003) 351.

[6] S. Obbade, C. Dion, M. Saadi, F. Abraham, J. Solid State Chem. 177 (2004) 1567.

[7] S. Obbade, C. Dion, M. Saadi, S. Yagoubi, F. Abraham, J. Solid State Chem. 177 (2004) 3909.

[8] S. Obbade, C. Dion, M. Rivenet, M. Saadi, F. Abraham, J. Solid State Chem. 177 (2004) 2058.

[9] P.S. Halasyamani, R.J. Francis, S.M. Walker, D. O'Hare, Inorg. Chem. 38 (1999) 271.

[10] S.V. Krivovichev, P.C. Burns, J. Solid State Chem. 170 (2003) 106.

[11] S.V. Krivovichev, C.L. Cahill, E.V. Nazarchuk, P.C. Burns, T. Armbruster, W. Depmeier, Microporous Mesoporous Mater. 78 (2005) 209.

[12] S.V. Krivovichev, P.C. Burns, T. Armbruster, E.V. Nazarchuk, W. Depmeier, Microporous Mesoporous Mater. 78 (2005) 217.

[13] S.V. Krivovichev, T. Armbruster, D.Y. Chernyshov, P.C. Burns, E.V. Nazarchuk, W. Depmeier, Microporous Mesoporous Mater. 78 (2005) 225.

[14] R.J. Francis, J. Drewitt, P.S. Halasyamani, C. Ranganathachar, D. O'Hare, W. Clegg, S.J. Teat, Chem. Commun. (1998) 279.

[15] J.A. Danis, W.H. Runde, B. Scott, J. Fettinger, B. Eichhorn, Chem. Commun. (2001) 2378.

[16] J.A. Danis, H.T. Hawkins, B.L. Scott, W.H. Runde, B.E. Scheetz, B.W. Eichhorn, Polyhedron 19 (2000) 1551.

[17] A.J. Locock, P.C. Burns, J. Solid State Chem. 177 (2004) 2675.

[18] M.B. Doran, C.L. Stuart, A.J. Norquist, D. O'Hare, Chem. Mater. 16 (2004) 565.

[19] M. Doran, S.M. Walker, D. O'Hare, Chem. Commun. (2001) 1988.

[20] S.V. Krivovichev, V. Kahlenberg, I.G. Tananaev, R. Kaindl, E. Mersdorf, B.F. Myasoedov, J. Am. Chem. Soc. 127 (2005) 1072.

[21] P.M. Almond, T.E. Albrecht-Schmitt, Inorg. Chem. 42 (2003) 5693.

[22] M.B. Doran, A.J. Norquist, D. O'Hare, Inorg. Chem. 42 (2003) 6989.

[23] A.J. Norquist, M.B. Doran, P.M. Thomas, D. O'Hare, Dalton Trans. (2003) 1168.

[24] A.J. Norquist, M.B. Doran, P.M. Thomas, D. O'Hare, Inorg. Chem. 42 (2003) 5949.

[25] A.J. Norquist, M.B. Doran, D. O'Hare, Solid State Sci. 5 (2003) 1149.

[26] A.J. Norquist, P.M. Thomas, M.B. Doran, D. O'Hare, Chem. Mater. 14 (2002) 5179.

[27] M. Doran, A.J. Norquist, D. O'Hare, Chem. Commun. (2002) 2946.

[28] P.M. Thomas, A.J. Norquist, M.B. Doran, D. O'Hare, J. Mater. Chem. 13 (2003) 88.

[29] M.B. Doran, A.J. Norquist, C.L. Stuart, D. O'Hare, Acta Crystallogr. E60 (2004) m996;
M.B. Doran, A.J. Norquist, D. O'Hare, Acta Crystallogr. E59 (2003) m762;
M.B. Doran, A.J. Norquist, D. O'Hare, Acta Crystallogr. E59 (2003) m765;
M.B. Doran, A.J. Norquist, D. O'Hare, Acta Crystallogr. E59 (2003) m373;
C.L. Stuart, M.B. Doran, A.J. Norquist, D. O'Hare, Acta Crystallogr. E59 (2003) m446.

[30] A.J. Norquist, M.B. Doran, D. O'Hare, Inorg. Chem. 44 (2005) 3837.

[31] M.B. Doran, B.E. Cockbain, A.J. Norquist, D. O'Hare, Dalton Trans. (2004) 3810.

[32] X. Wang, J. Huang, A.J. Jacobson, J. Am. Chem. Soc. 124 (2002) 15190.

[33] R.J. Francis, P.S. Halasyamani, J.S. Bee, D. O'Hare, J. Am. Chem. Soc. 121 (1999) 1609.

[34] R.J. Francis, P.S. Halasyamani, D. O'Hare, Angew. Chem. Int. Ed. 37 (1998) 2214.

[35] S. Allen, S. Barlow, P.S. Halasyamani, J.F.W. Mosselmans, D. O'Hare, S.M. Walker, R.I. Walton, Inorg. Chem. 39 (2000) 3791.

[36] R.J. Francis, P.S. Halasyamani, D. O'Hare, Chem. Mater. 10 (1998) 3131.

[37] S.M. Walker, P.S. Halasyamani, S. Allen, D. O'Hare, J. Am. Chem. Soc. 121 (1999) 10513.

[38] C.L. Cahill, P.C. Burns, Inorg. Chem. 40 (2001) 1347.

[39] P.S. Halasyamani, S.M. Walker, D. O'Hare, J. Am. Chem. Soc. 121 (1999) 7415.

[40] A.M. Chippindale, R.L. Walton, J. Chem. Soc. Chem. Commun. (1994) 2453.

[41] A.M. Chippindale, A.R. Cowley, R.L. Walton, J. Mater. Chem. 6 (1996) 611.

[42] J.C. Trombe, P. Thomas, C. Brouca-Cabarrecq, Solid State Sci. 3 (2001) 309.

[43] Z. Bircsak, W.T.A. Harrison, Acta Crystallogr. C54 (1998) 1383.

[44] F. Fourcade-Cavillou, J.C. Trombe, Solid State Sci. 4 (2002) 1199.

[45] M. Saadi, Thesis, Lille, France, 1994.

[46] SAINT Plus Version 6.22, Bruker Analytical X-ray Systems, Madison, WI, 2001.

[47] SADABS Version 2.03: Bruker Analytical X-ray Systems, Madison, WI, 2001.

[48] A. Altomare, G. Cascaro, G. Giacovazzo, A. Guargliardi, M.C. Burla, G. Polidori, M. Gamalli, J. Appl. Crystallogr. 27 (1994) 135.

[49] V. Petricek, M. Dusek, L. Palatinus, JANA2000, Institute of Physics, Praha, Czech Republic, 2005.

[50] C. Frondel, D. Riska, J.W. Frondel, US Geol. Surv. Bull. 1036-G (1956) 91.

[51] M. Saadi, Thesis, El Jadida, Morocco, 2001.

[52] F. Cesbron, Bull. Soc. Fr. Minéral. Cristallogr. 93 (1973) 320.

[53] P.C. Burns, R.C. Ewing, F.C. Hawthorne, Can. Miner. 35 (1997) 1551.

[54] F. Abraham, C. Dion, M. Saadi, J. Mater. Chem. 3 (5) (1993) 459.

[55] R. Enjalbert, J. Galy, Acta Crystallogr. C42 (1986) 1467.

[56] K.H. Tytko, J. Mehmke, D. Kurad, Struct. Bonding 93 (1999) 1.

[57] M. Gasperin, Acta Crystallogr. C43 (1987) 404.

[58] A.J. Locock, S. Skanthakumar, P.C. Burns, L. Soderholm, Chem. Mater. 16 (2004) 1384.

[59] P.C. Burns, M.L. Miller, R.C. Ewing, Can. Mineral. 34 (1996) 845; P.C. Burns, Can. Mineral. 43 (2005) 1839.

[60] A.J. Locock, P.C. Burns, J. Solid State Chem. 176 (2003) 18.

[61] R.D. Shannon, Acta Crystallogr. A32 (1976) 751.

[62] A.A. Khan, W. Baur, Acta Crystallogr. B28 (1972) 683.

[63] N. Tancret, S. Obbade, F. Abraham, Eur. J. Solid State Inorg. Chem. 32 (1995) 195; A.M. Chippindale, P.J. Dickens, G.J. Flynn, G.P. Stuttard, J. Mater. Chem. 5 (1995) 141.